Mechanics Research Communications 38 (2011) 106–110

Contents lists available at ScienceDirect

Mechanics Research Communications

journal homepage: www.elsevier.com/locate/mechrescom

Acoustic emission for fatigue damage characterization in metal plates

D.G. Aggelis*, E.Z. Kordatos, T.E. Matikas

Department of Materials Science and Engineering, University of Ioannina, Ioannina 45110, Greece

ARTICLE INFO

Article history:
Received 27 July 2010
Received in revised form 4 January 2011
Available online 20 January 2011

Keywords:
Aluminium
Nondestructive testing
Fracture mode

ABSTRACT

Acoustic emission (AE) supplies information on the fracturing behavior of different materials. In this study, AE activity was recorded during fatigue experiments in metal coupons. The plates were characterized by a symmetric V-shape notch and were loaded in tension–tension fatigue until final failure with concurrent AE activity monitoring. The relatively broad bandwidth of the sensors enabled the recording of a wide range of frequencies up to 1 MHz. AE parameters like energy and duration exhibited a certain increase with the accumulation of damage although the hit rate was not significantly influenced. Furthermore the behavior of RA value (ratio of rise time to amplitude of the waveforms) which quantifies the shape of the first part of the AE signals and has been used for characterization of the cracking mode, showed a certain shift indicating the transition from tensile mode to shear which can be confirmed by the visual observation of the crack geometry after the experiment. The time history of RA is similar to the crack propagation rate (da/dN) curve but exhibits the rapid hyperbolic growth consistently about 1000 cycles earlier than final failure. Therefore, the use of acoustic emission parameters is discussed both in terms of characterization of the damage mechanisms, as well as a tool for the prediction of ultimate life of the material under fatigue.

1. Introduction

Acoustic emission (AE) is a method widely used for real time monitoring of the structural condition of materials and structures. It utilizes the elastic energy released from any crack propagation incident. This energy propagates through the material in the form of stress waves and can be detected by suitable sensors on the surface (Grosse and Ohtsu, 2008; Mindess, 2004). The cumulative AE activity, as recorded by the sensors is indicative of the severity of cracking, since crack propagation is a prerequisite for AE. High rate of incoming signals implies the existence of several active source cracks, while low or zero activity is connected to healthy material. When several sensors are used, apart from the number of AE signals (hits), the geometric location of the cracks can be extracted due to the delay between the reception of the wave at the different measurement points (Aggelis et al., 2009; Grosse et al., 1997). This allows the estimation of which part of the structure has suffered more extensive deterioration in order to take the necessary repair action, especially for large scale structures (Yuyama et al., 2007).

However, there are other important aspects of AE measurements, which are based on qualitative parameters of the received signals. The waveform shape depends on the cracking mode, enabling the classification of cracks in different materials (Anastassopoulos and Philippidis, 1994; Ohtsu and Tomoda, 2007; Shiotani et al., 2001). Shear cracks generally follow tensile as the material approaches to final failure. Therefore, crack characterization may lead to an early warning. In general, when a tensile event is occurring, the sides of the cracks move away from each other, leading to a transient volumetric change of the material and consequently most of the energy is transmitted in the form of longitudinal waves, while only a small amount in shear waves which propagate on a lower velocity. Therefore, most of the energy is recorded quite early within the received waveform. Fig. 1 shows an example of AE waveform emitted by a tensile event. The delay between the onset and the highest peak (called rise time, RT), is short leading to a high rise angle of the wave. In case of a shear crack, the shape (and not the volume) of the material near the crack vicinity changes, shifting the proportion of energy in favor of the shear waves. Therefore, the most important part of the waveform arrives much later than the fast longitudinal arrivals, leading to longer RT and consequently small rise angle, as seen in the right of Fig. 1. Recently the shape of the initial part of the waveform is examined by the RA value which is defined as the RT over the amplitude, A and is measured in μs/V (or ms/V), as suggested by relevant recommendations (Rilem, 2009). Additionally, tensile events are characterized by higher frequency content, as expressed by the average frequency (AF) defined by the number of threshold crossings over the signal duration (Rilem, 2009). It is mentioned that the measurements depend on the "threshold" which is a value set by the user high enough in order to avoid low environmental or other noise, but at

* Corresponding author. Tel.: +30 26510 08006; fax: +30 26510 08054.
E-mail addresses: daggelis@cc.uoi.gr, aggelis_d@yahoo.com (D.G. Aggelis).

0093-6413/$ – see front matter © 2011 Elsevier Ltd. All rights reserved.
doi:10.1016/j.mechrescom.2011.01.011

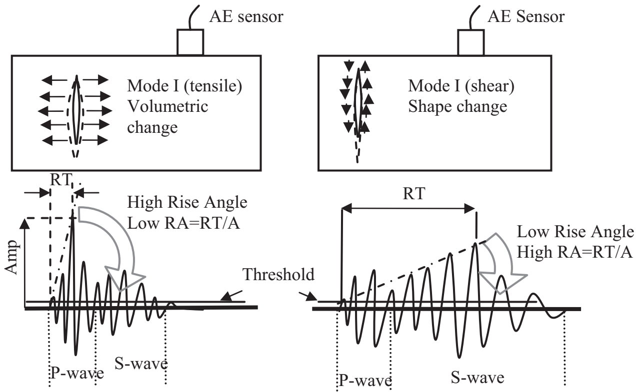

Fig. 1. Cracking modes and corresponding AE signals.

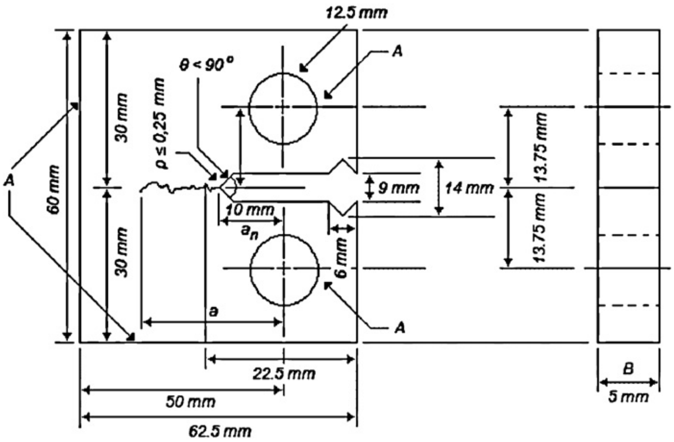

Fig. 2. Specimen geometry.

the same time sensitive enough to allow recording of the actual AE hits due to crack propagation or other material processes.

This classification scheme has proven powerful in case of laboratory applications concerning concrete cracking due to corrosion of metal reinforcing bar (Ohtsu and Tomoda, 2007), fracture of composite laminates (Anastassopoulos and Philippidis, 1994; Aggelis et al., 2010), as well as the discrimination between matrix cracking and pull out during bending of fibre reinforced concrete (Soulioti et al., 2009) or concrete with large metal rebars (Ohno and Ohtsu, 2010). Specifically for the field of metals, mainly the cumulative AE activity is utilized, being related to strength in single fibre fragmentation tests (Rousset et al., 2009), as well as to the remaining life in fatigue tests of steel specimens with notches (Roberts and Talebzadeh, 2003a,b). AE has also been used to clarify the moment of crack nucleation in indentation experiments (Yonezu et al., 2010). Amplitude and cumulative activity have been monitored during bending of metal composite foams (Brown et al., 2010), while, concerning aluminium, AE parameters like rise time and duration have been considered in an attempt to correlate with corrosive processes (Boinet et al., 2010).

In this study aluminium specimens with notches were fractured in fatigue tests. Measurements of the crack propagation rate were conducted with simultaneous AE monitoring in order to correlate the parameters obtained nondestructively with mechanical results and propose certain features as the most promising for fatigue damage characterization in metals.

2. Experimental procedure

2.1. Materials and mechanical testing

The material was aluminium (AA 7075). This material (aluminium and its alloys) exhibits good resistance to corrosion, and high strength in environment as well as high temperatures. This study mainly intends to present the acoustic emission behavior during the tests, but for the interested reader, the chemical composition and the mechanical properties of the material, including tensile strength and hardness are presented in Tables 1 and 2, respectively, as supplied by the manufacturer.

Test specimens were manufactured according to ASTM E399-09e1. The geometry of the specimen is shown in Fig. 2.

For the determination of the crack propagation rate (CPR) a crack opening displacement (COD) meter is fixed in the notch opening. The determination of crack propagation rate followed ASTM E647-08e1. The fatigue tests were conducted on an INSTRON servo-hydraulic machine with maximum static and dynamic load of ±100 kN. The fatigue cycle was sinusoidal with frequency of

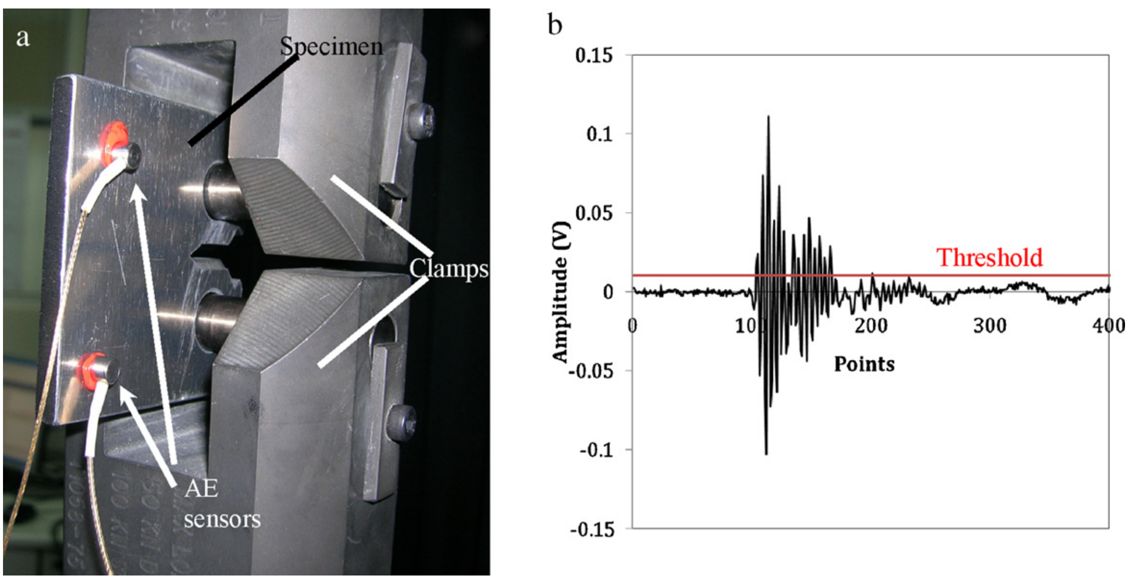

Fig. 3. (a) Photograph of the sensors on the specimen and (b) Real typical waveform with threshold.

Table 1
Chemical composition of AA 7075.

Material	Elements (wt%)							
	Cu	Si	Zn	Pb	Fe	Mg	Mn	Ti
AA 7075 En 573-3 (AlZnMgCu1, 5F53)	1.20–2.00	Max–0.40	5.10–6.10	1.00–2.50	Max–0.50	2.10–2.90	Max–0.30	Max–0.20

Table 2
Mechanical properties of AA 7075.

Material	$\sigma_{0.2}$ (MPa)	σ_{uts} (MPa)	ε (%)	HV_{10}
AA 7075 En 573-3 (AlZnMgCu1, 5F53)	460	530	5	158

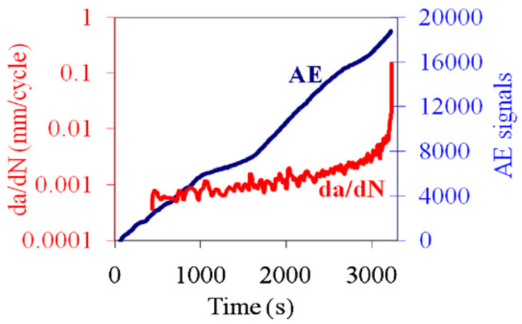

Fig. 4. Time history of CPR and cumulative AE.

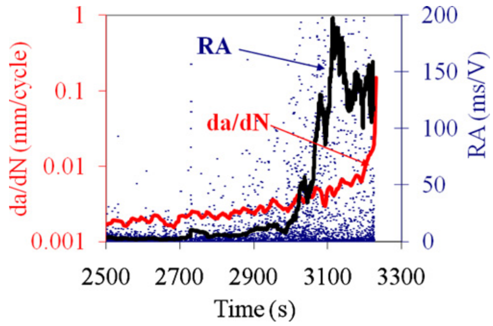

Fig. 6. Time history of CPR and RA.

3 Hz, stress ratio (minimum to maximum) $R = 0.2$ and amplitude 4 kN.

2.2. Acoustic emission

Two piezoelectric sensors (Pico, Physical Acoustics Corp., PAC) were attached on one side of the specimen (see Fig. 3a). The sensors were attached using wax, which enhanced acoustic coupling, while supporting the sensors throughout the experiment. The frequency bandwidth is within 50–800 kHz and therefore, the sensors are suitable for monitoring of different sources. The AE signals were recorded by two channels in a PCI-2 board, PAC with a sampling rate of 5 MHz. The software used was AE Win, PAC, while acoustic activity appeared in real time, as well as most of the signal parameters. The whole data were recorded for post-processing. The threshold was set to 40 dB (or 0.01 V, see Fig. 3b).

3. Results

Fig. 4 shows the crack propagation rate (da/dN) as a function of time. As typically expected in metal fatigue the rate increases exponentially. The final failure of the specimen occurred at 3231 s. AE monitoring presented a more or less constant activity throughout the experiment. A typical example is again seen in Fig. 4. AE signals are recorded shortly after the start of the test. Without much fluctuations, the AE hit rate can be characterized as constant leading to a total number of almost 20,000 hits.

However, the qualitative parameters of AE show a very distinct and clear trend. Fig. 5 presents the duration and rise time of the signals. Each point on the graph represents the duration or rise time of the specific hit. It is clear that approximately 200–300 s before the final fracture, the duration and RT start to increase sharply. Specifically, until before 3000 s the duration of the acquired signals was typically less than 3000 μs, while the RT less than 500 μs; after that point, AE signals with much longer duration and RT are recorded, as seen by the cloud of points rising to the top of the figure before the final fracture.

The increasing duration and RT indicate possible shift of the cracking mode from tensile to shear. As mentioned above, this transition between different cracking modes can be examined by the RA value (Rilem, 2009) which also takes into account the signals' amplitude. RA history in relation to the CPR can be seen in Fig. 6 for the last stage of the specimen's life (after 2500 s).

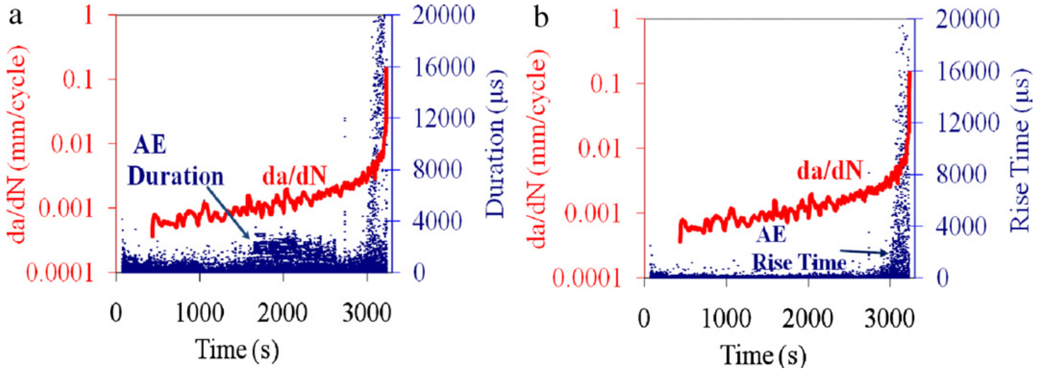

Fig. 5. Time history of CPR and (a) AE duration and (b) RT.

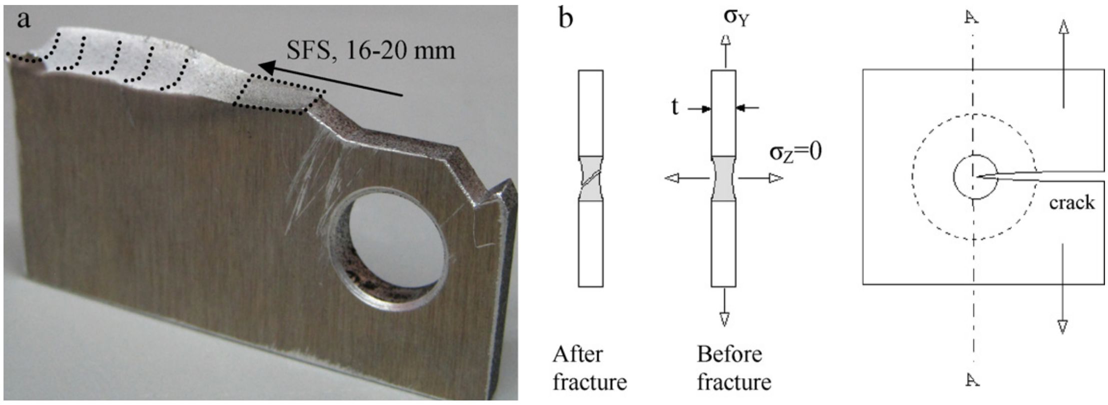

Fig. 7. (a) Part of the specimen after fatigue failure. (b) Plane stress fracture.

Before 2700 s RA values higher than 50 ms/V are rare. Between 2700 s and 2900 s hits with RA between 50 and 100 ms/V appear, while after 2900 s the population of points expands to values higher than 100 ms/V. The solid line stands for the moving average of the recent 150 hits, which shows a clear increase at 3000 s, much earlier than the specimen's final fracture. As discussed above, this shift of the RA value implies also the shift between the tensile and shear fracture modes; actually this is the sequence of the cracking modes within a typical fatigue specimen of this kind. Fig. 7a shows a photograph of the fracture surface after the end of the experiment.

The distance between the notch and the point of load application is 10 mm (as was seen in Fig. 2). This is considered to be the initial crack length. The crack propagates horizontally, creating a straight fracture surface (SFS) for an additional 5–10 mm away from the notch. Later, the fracture surface becomes curved. This is attributed to the local plane stress field. Due to the small thickness of the plate, the stress perpendicular to the surface (σ_Z) is zero (Fig. 7b). Therefore, although the crack starts to propagate horizontally dictated by the notch, under the application of the tensile stress (σ_Y), final fracture occurs due to the shear stresses, which are maximum at

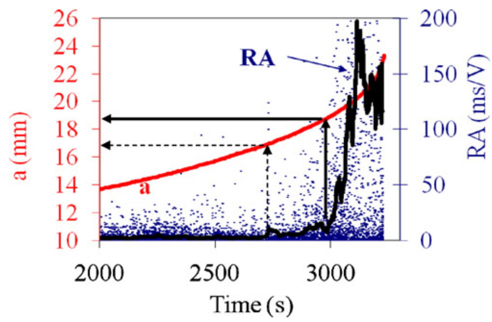

Fig. 8. Time history of crack length a and RA value.

45°. This cracking mode sequence may well be one reason behind the shifting behavior of the AE parameters. The small specimen size and the sensitivity of the sensors, enable capturing these changes accurately as the crack develops.

Fig. 8 shows the total length of the crack for the same specimen along with the RA value vs. time. When RA starts to exhibit

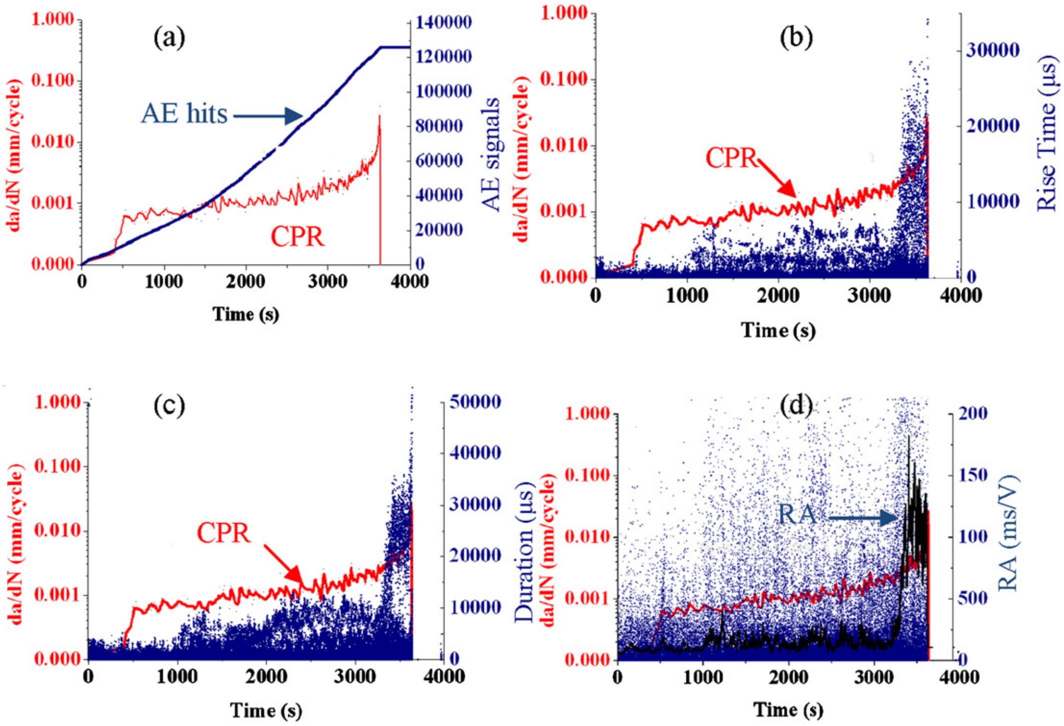

Fig. 9. Time history of CPR and (a) AE hits, (b) rise time, (c) duration, and (d) RA.

the clear increasing tendency (before 3000 s, indicated by a vertical arrow), the total length of crack is almost 19 mm. Additionally, a low local maximum of the curve at approximately 2750 s (indicated by dash line arrows), can be regarded as the first sign of RA increase and occurs at the crack length of 16.8 mm. These coincide with the length of the straight fracture surface (SFS) of the crack in Fig. 7a, before the cracked area becomes curved. This observation supports the assumption that the change in RA values is due to the shift of the dominant failure mode from tension to shear.

The AE behavior is repeatable for all three specimens tested. Fig. 9 shows the cumulative AE hits, RT, duration and RA value for another aluminium specimen. In this case the AE rate remains constant as well, while the other shape parameters exhibit the same increasing trend. The specimen failed at 3636 s, while the parameters undergo an increase from about 3200 s.

The above results imply that for a similar experimental procedure (material, specimen geometry, fatigue parameters) when RA exhibits a sharp increase this would indicate a remaining life of approximately 1000 cycles. Although this trend is consistent for the specific experimental series, it needs to be further studied and verified in other types of materials, specimen sizes and general experimental conditions. This would lead to more robust conclusions regarding the possibility of prediction of the final failure of metals subjected to fatigue. Additionally different aspects of the acoustic emission testing should be revisited. The population of hits is huge, possibly including redundant data, while proper filtering of the hits would clear the trends. It is even possible that at the last stage of the experiment, the emissions are so frequent that different signals overlap and are recorded as one. This may contribute to the increased duration of the signals, which in any case indicates the switch of the fracture mode.

4. Conclusion

This paper presents some preliminary results on the acoustic emission monitoring during fatigue of aluminium coupons. The aim is the correlation of AE parameters with damage accumulation and the fracture mode. Study of the AE behavior shows that certain characteristics undergo clearly measurable changes much earlier than final fracture. Specifically, among others, the duration and the rise time of the signals, as well as the RA value of the waveforms increase sharply approximately 1000–1200 cycles before final failure. The mechanism which is responsible for this change in acoustic emission seems to be the shift between the tensile and the shear fracture modes which typically occurs in thin metal coupons with a notch. This is supported by visual observation of the specimen's surface after fracture. In any case, independent of the specific reason behind the AE behavior, it is concluded that AE parameters (apart from the total activity) are sensitive to the damage process and should be further studied in order to lead to early warning against final fracture and characterization of the damage status at any point of the materials life.

References

Aggelis, D.G., Barkoula, N.M., Matikas, T.E., Paipetis, A.S., 2010. Acoustic emission monitoring of degradation of cross ply laminates. The Journal of the Acoustical Society of America 127 (6), EL246–251.

Aggelis, D.G., Shiotani, T., Momoki, S., Hirama, A., 2009. Acoustic emission and ultrasound for damage characterization of concrete elements. ACI Materials Journal 106 (6), 509–514.

Anastassopoulos, A.A., Philippidis, T.P., 1994. Clustering methodology for evaluation of acoustic emission from composites. Journal of Acoustics Emission 13 (1/2), 11–22.

Boinet, M., Bernard, J., Chatenet, M., Dalard, F., Maximovitch, S., 2010. Understanding aluminium behaviour in aqueous alkaline solution using coupled techniques. Part II: acoustic emission study. Electrochimica Acta 55, 3454–3463.

Brown, J.A., Vendra, L.J., Rabiei, A., 2010. Bending properties of al-steel and steel-steel composite metal foams. Metallurgical and Materials Transactions A 41 (11), 2784–2793.

Grosse, C.U., Ohtsu, M., 2008. Acoustic Emission Testing. Springer, Heidelberg.

Grosse, C., Reinhardt, H., Dahm, T., 1997. Localization and classification of fracture types in concrete with quantitative acoustic emission measurement techniques. NDT&E International 30 (4), 223–230.

Mindess, S., 2004. Acoustic emission methods. In: Malhotra, V.M., Carino, N.J. (Eds.), CRC Handbook of Nondestructive Testing of Concrete. CRC, Boca Raton, FL.

Ohno, K., Ohtsu, M., 2010. Crack classification in concrete based on acoustic emission. Construction and Building Materials 24, 2339–2346.

Ohtsu, M., Tomoda, Y., 2007. Phenomenological model of corrosion process in reinforced concrete identified by acoustic emission. ACI Materials Journal 105 (2), 194–200.

RILEM Technical Committee 212-ACD, 2009. Acoustic emission and related NDE techniques for crack detection and damage evaluation in concrete (2004–2009). Available from: http://www.rilem.net/tcDetails.php?tc=212-ACD.

Roberts, T.M., Talebzadeh, M., 2003a. Acoustic emission monitoring of fatigue crack propagation. Journal of Constructional Steel Research 59, 695–712.

Roberts, T.M., Talebzadeh, M., 2003b. Fatigue life prediction based on crack propagation and acoustic emission count rates. Journal of Constructional Steel Research 59, 679–694.

Rousset, G., Martin, E., Lamon, J., 2009. In situ fibre strength determination in metal matrix composites. Composite Science and Technology 69, 2580–2586.

Shiotani, T., Ohtsu, M., Ikeda, K., 2001. Detection and evaluation of AE waves due to rock deformation. Construction and Building Materials 15 (5–6), 235–246.

Soulioti, D.V., Barkoula, N.M., Paipetis, A.S., Matikas, T.E., Shiotani, T., Aggelis, D.G., 2009. Acoustic emission behaviour of steel fibre reinforced concrete under bending. Construction and Building Materials 23, 3532–3536.

Yonezu, A., Arino, M., Kondo, T., Hirakata, H., Minoshima, K., 2010. On hydrogen-induced Vickers indentation cracking in high-strength steel. Mechanics Research Communications 37, 230–234.

Yuyama, S., Yokoyama, K., Niitani, K., Ohtsu, O., Uomoto, T., 2007. Detection and evaluation of failures in high-strength tendon of prestressed concrete bridges by acoustic emission. Construction and Building Materials 21, 491–500.